SUPPLEMENTAL INFORMATION

INVENTORY OF SUPPLEMENTAL ITEMS

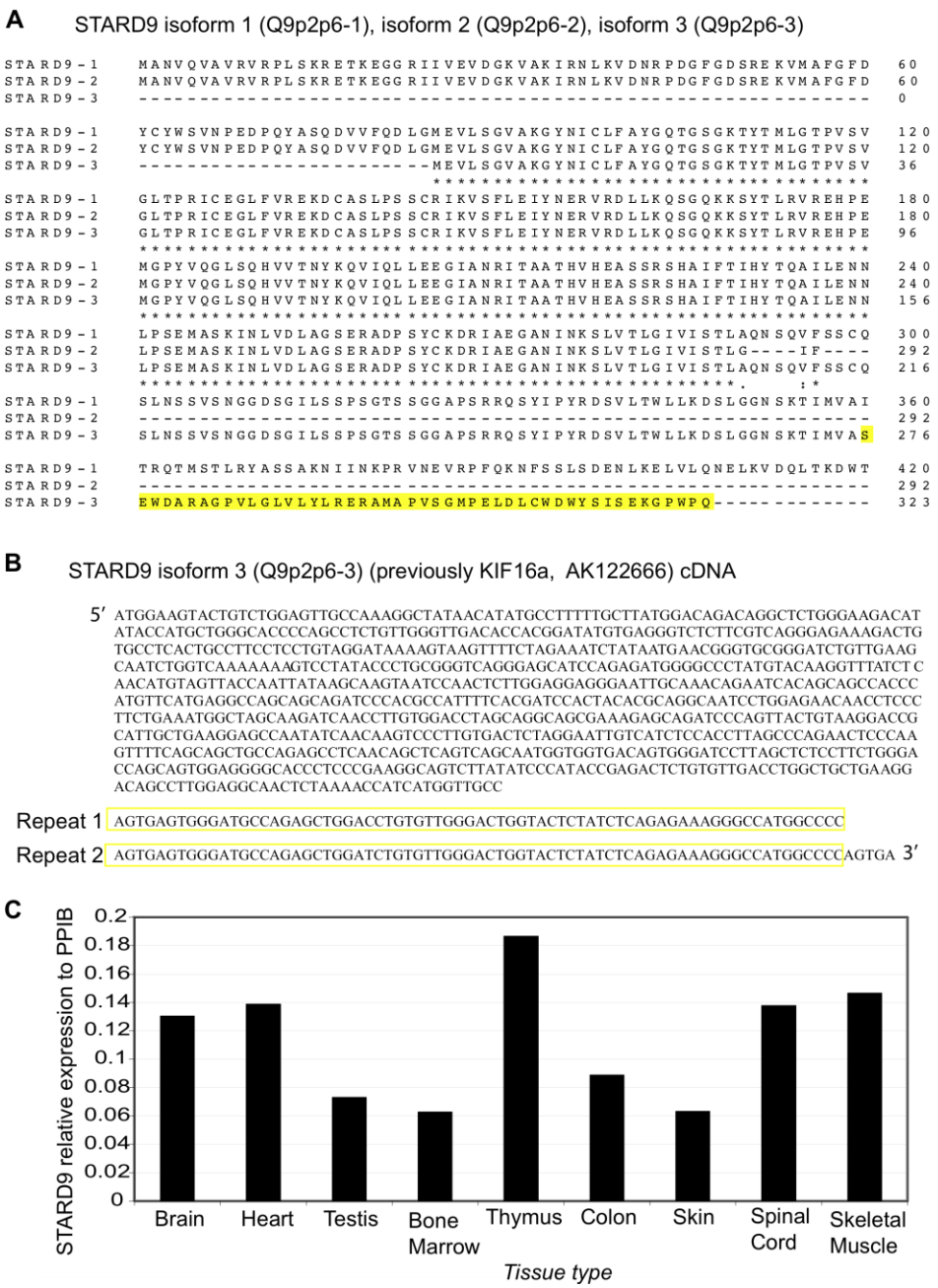

Figure S1. STARD9 Isoforms and Tissue Expression, Related to Figure 3

STARD9 isoform alignments. (A) Sequence alignment of the first 420 amino acids of STARD9 isoform 1 (Q9p2p6-1) and complete isoforms 2 (Q9p2p6-2) and 3 (Q9p2p6-3). Note isoform 3 is missing the first 84 amino acids predicted to be essential for ATPase activity. Also note, isoform 2 is only 292 amino acids and lacks a portion of the motor domain. Highlighted residues are encoded by repetitive DNA sequences in (B). (B) cDNA sequence predicted to encode Q9p2p6-3/AK12266/Kif16a. Boxed nucleotides indicate repeats at the 3'end of the cDNA, predicted to encode for highlighted residues in (A). (C) The STARD9 gene is ubiquitously expressed at low levels across various tissues. STARD9 gene expression levels relative to the PPIB gene were quantified by using 500 ng of mRNA from indicated tissues in the QuantiGene gene expression system (Panomics) (see Supplemental Experimental Procedures).

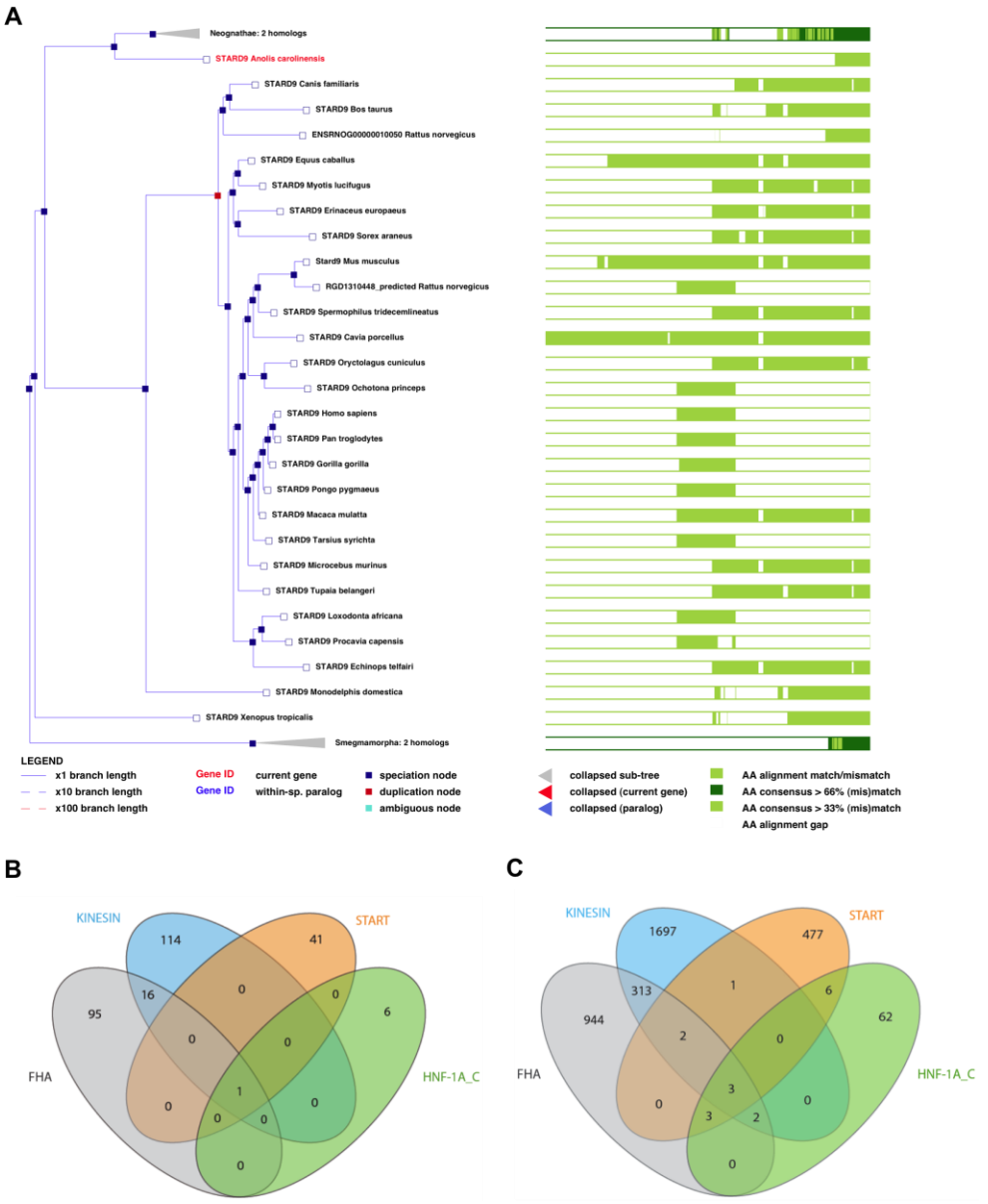

Figure S2. STARD9 Orthologs, Related to Figure 3

(A) The STARD9 gene tree was generated by Ensembl (http://www.ensembl.org/Homo_sapiens/Gene/Compara_Tree?db=core;g=ENSG00000159433;r=15:40766990-40800348;t=ENST00000290607), using the Gene Orthology/Paralogy prediction method pipeline (Vilella et al., 2009) for all proteins and species in the Ensembl database. (B) Proteins sharing the domain architecture of STARD9 were found by querying several databases either for sequences with strong similarity to, or those that contain domains in common with human STARD9. The Unison database was surveyed for all proteins from the manually annotated and reviewed (Swiss-Prot) subset of UniProtKB (http://www.uniprot.org) that shared at least one Pfam domain in common with human STARD9. The degree to which these proteins share domain architecture with STARD9 is shown in the Venn diagram. Although human STARD9 is the only protein in this set that contains both Kinesin motor and START domains, similar analyses (C) that include non-curated, predicted protein sequences identify putative orthologs from cow (XP_602450.4) and dog (XP_544643.2) in the set of proteins sharing three of four domains with the human protein.

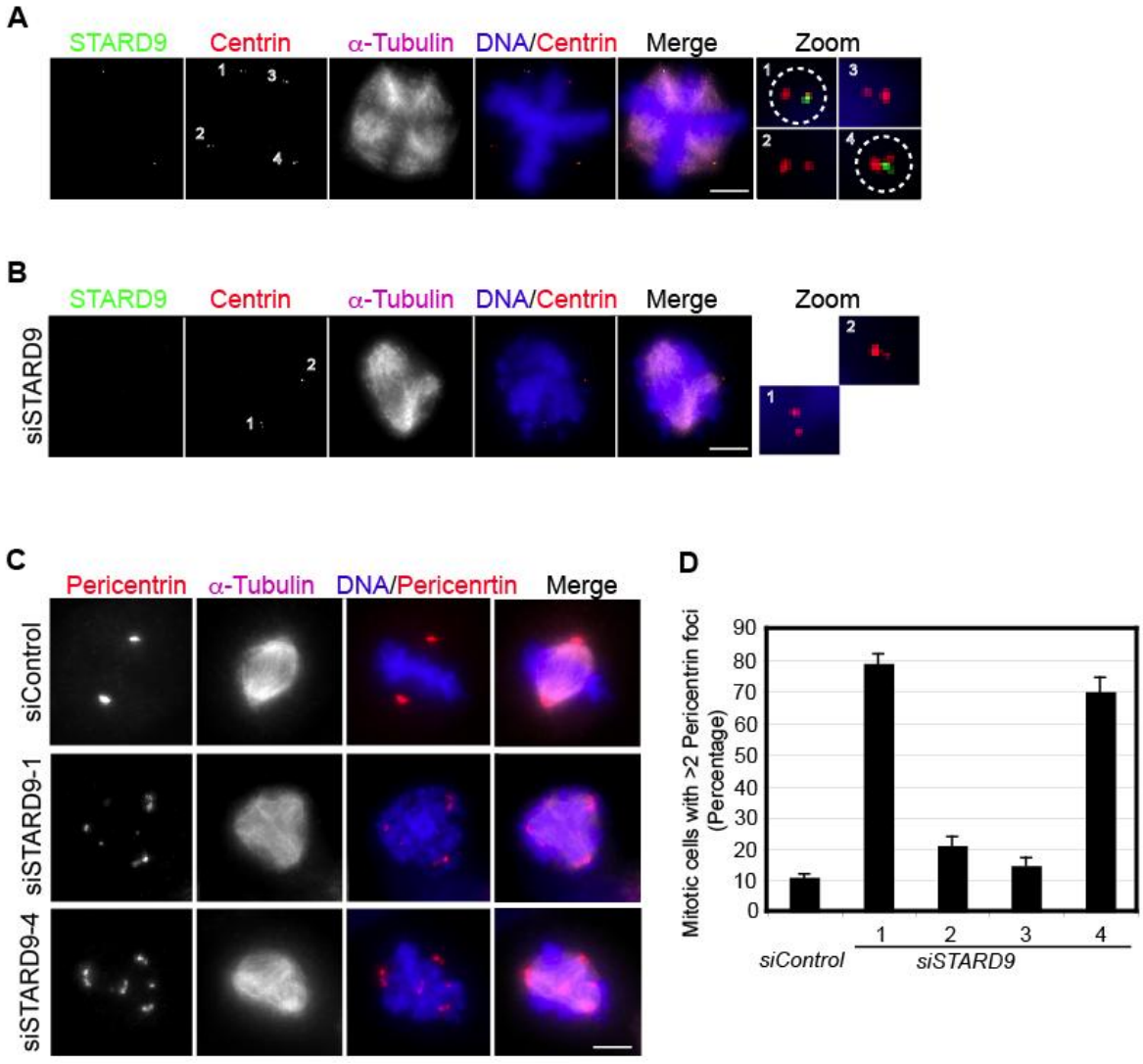

Figure S3. STARD9 Localization and Depletion Phenotype, Related to Figures 3 and 5

STARD9 Localization (A) STARD9 localizes only to two daughter centrioles in cells with more than two centrosomes. HeLa cells were fixed and stained for STARD9, centrin, and α-tubulin. Zoom panel shows centriole pairs numbered 1-4, note STARD9 only localizes to two daughter centrioles in two centrosomes, indicated by dotted circles. (B) STARD9 is depleted form centrosomes upon RNAi-treatment. STARD9-depleted HeLa cells were fixed and stained as in A. Zoom panel shows two centriole pairs lacking STARD9 staining. (C) Multiple siRNA oligonucleotides targeting STARD9 display similar phenotypes, including PCM fragmentation and multipolar spindle formation. For A, B and C, bar = 5 μm. (D) The percentage of mitotic cells with greater than two pericentrin foci were quantified for siControl and siSTARD9 oligos 1 through 4.

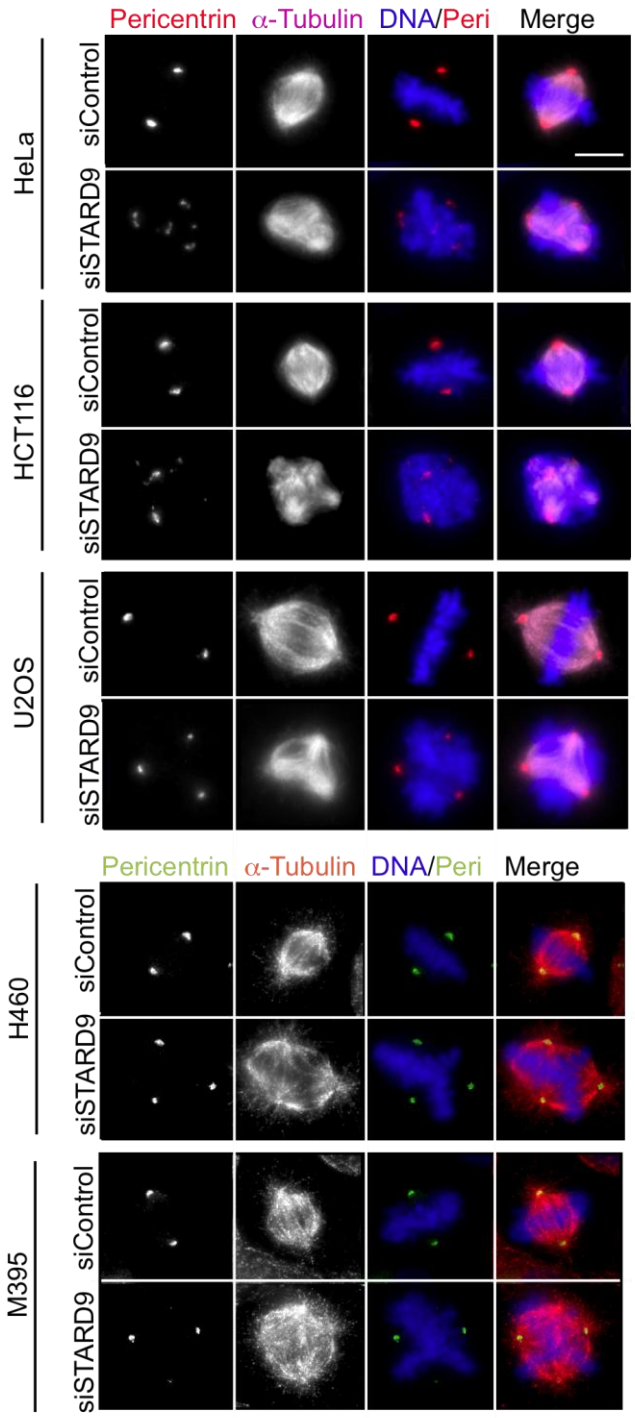

Figure S4. The STARD9-depletion Phenotype is Conserved Among Multiple Cancer Cell Lines, Related to Figure 5

Depletion of STARD9 leads to PCM fragmentation and spindle defects in multiple cancer cell lines. (A) HeLa, HCT116, U2OS, H460, and M395 cell lines were treated with control or STARD9 siRNA for 48 hours. Cells were fixed and stained for DNA, α-tubulin and pericentrin. Bar = 5 μm.

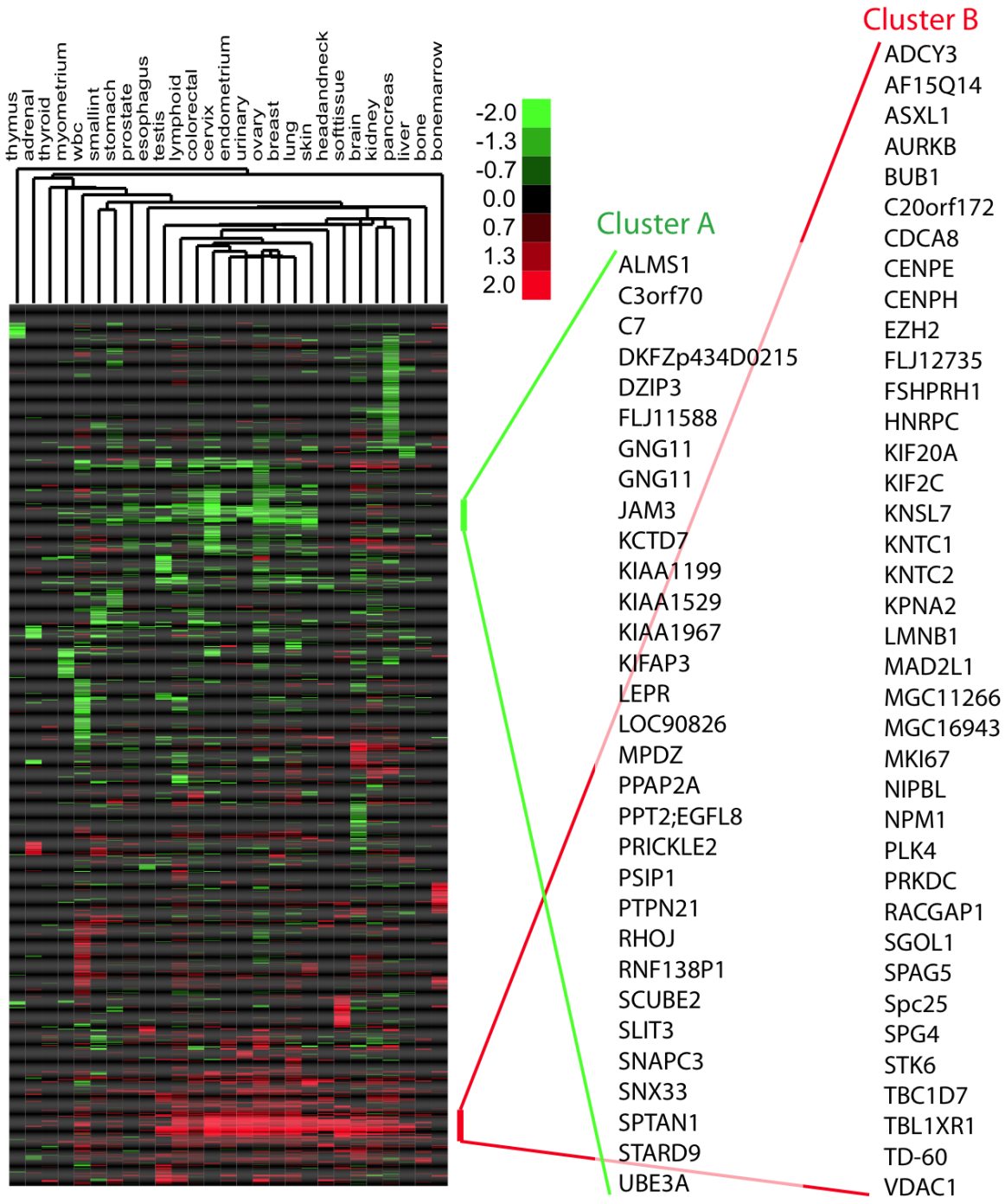

Figure S5. Gene Expression Analysis of MMCPs in Cancer, Related to Figure 5
Heat map summarizing differential gene expression levels of genes in the mitotic microtubule co-purifying protein set across 27 cancer tissues versus normal samples from the same tissue. Each tissue type is represented by 20 to > 100 cancer and 2 to 20 normal samples. Log (base 2) expression ratios were clustered hierarchically along both probe and tissue axes. Red represents gene over-expression, green under-expression, and black no significant change in expression, for cancer relative to normal samples. Cluster A represents genes under-expressed across multiple cancer types. Cluster B represents genes over-expressed across multiple cancer types.

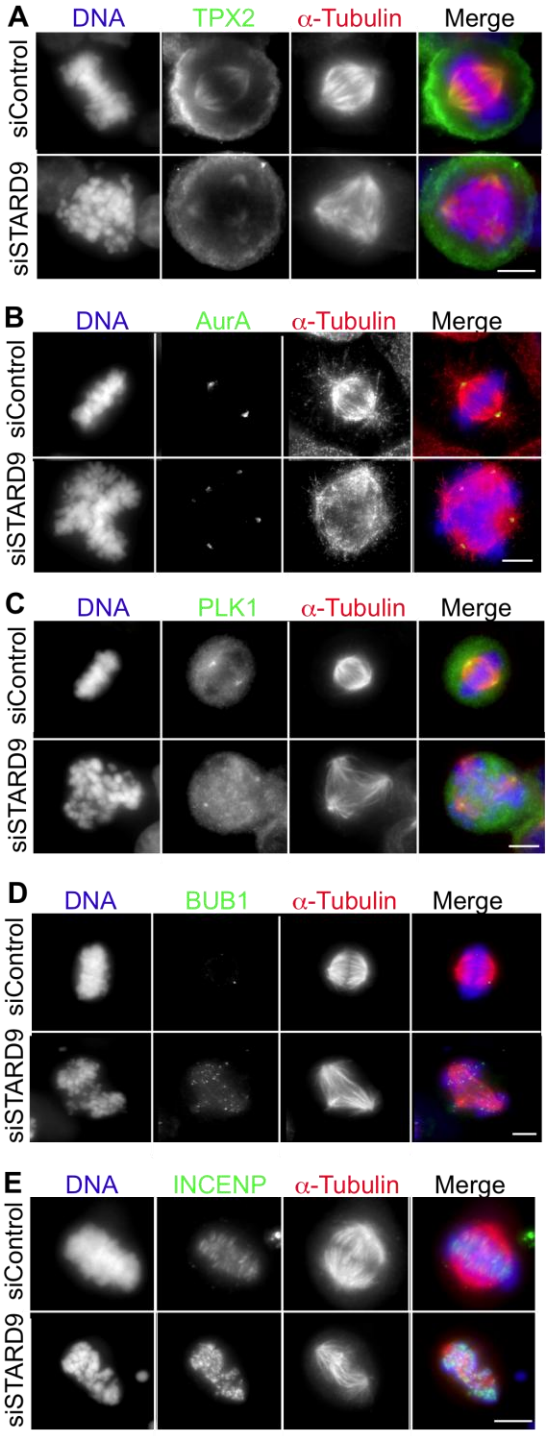

Figure S6. Localization of Spindle Assembly Proteins in STARD9-depleted Cells, Related to Figure 6

(A-D) HeLa cells were treated with control or STARD9 siRNA for 48 hours. Cells were fixed and stained for DNA, α-tubulin and TPX2 (A), Aurora A (B), Plk1 (C), Bub1 (D), or INCENP (E). (A) STARD9 is not required for proper localization of spindle pole focusing proteins. (B) Plk1 localizes predominantly to two spindle poles in multipolar siSTARD9 cells. (C-D) Spindle assembly checkpoint (SAC) proteins remain localized to kinetochores of non-congressed chromosomes in siSTARD9 cells. Bar = 5 μm.

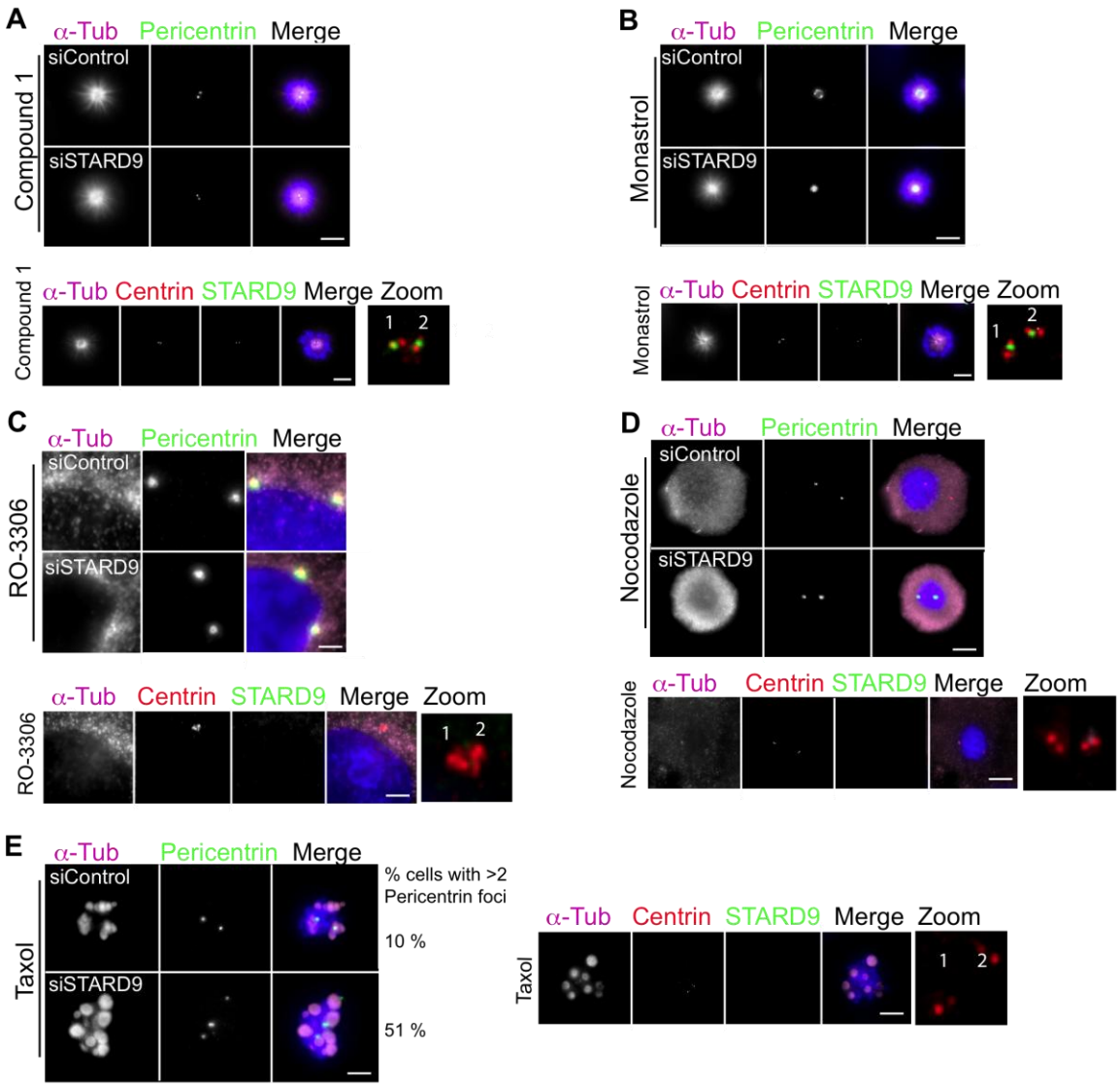

F

	STARD9 Localization	PCM Fragmentation						
		Untreated	Vehicle	Compound 1	Mon	RO-3306	Tax	Noc
siControl	+	-	-	-	-	-	-	-
siSTARD9	-	+	+	-	-	-	+	-
Vehicle	+	-						
Compound1	+	-						
Monastrol	+	-						
RO-3306	-	-						
Taxol	-/+	-/+						
Nocodazole	-	-						

Figure S7. Chemical Inhibition of Cdk1, Plk1, or Kinesin-5 Function Prevents PCM Fragmentation in STARD9-depleted Cells, Related to Figure 7

(A-F) 18 hours post-transfection, control or STARD9 siRNA-treated HeLa cells were arrested in G1/S with 2 mM Thymidine for 18 hours, washed, and released. Indicated small molecules were added 5 hours post release and cells were fixed and stained with indicated antibodies 4 hours post small molecule addition. (A) Compound 1 (Plk1

inhibitor) treatment arrests cells with a monopolar spindle. Upper panel, compound 1 treatment prevents PCM fragmentation in STARD9 siRNA treated cells. Lower panel, in compound 1 treated cells STARD9 localizes properly to the daughter centrioles. (B) Cells treated with monastrol (Kinesin-5 inhibitor) arrest with a monopolar spindle. Top panel, monastrol treatment prevents PCM fragmentation in STARD9 siRNA treated cells. Lower panel, in monastrol treated cells STARD9 localizes to the daughter centrioles. (C) RO-3306 (Cdk1 inhibitor) treated cells arrest at the G2/M transition. Upper panel, similar to control cells, siSTARD9 cells treated with RO-3306 show no increase in PCM fragmentation. Lower panel, STARD9 is absent from daughter centrioles in RO-3306 treated cells. (D) taxol (microtubule stabilizer) treated cells form ectopic sites of microtubule nucleation, leading to aster formation. Upper panel, compared to control cells, siSTARD9 cells treated with taxol have increased PCM fragmentation (10 % versus 51 %). Lower panel, STARD9 is absent from daughter centrioles in taxol treated cells. (E) Nocodazole (microtubule depolymerizer) treated cells arrest at the G2/M transition. Left panel, similar to control cells, no increase in PCM fragmentation is observed in nocodazole treated siSTARD9 cells. Right panel, STARD9 is absent from daughter centrioles in nocodazole-arrested cells. Bar = 5 μm. (F) Summary of STARD9 centriole localization and PCM fragmentation results from panels A-E. + sign indicates > 50%, - sign indicates ≤ 10%, and -/+ indicates ≥ 10%.

Table S1. Proteomic and *In Silico* Characterization of Mitotic Microtubule Co-purifying Proteins (MMCPs), Related to Figure 1

Excel file listing MMCPs identified by LC-MS/MS and accompanying information. NCBI RefSeq protein accession numbers, Gene Ontology GO terms, and literature-based functional categories are indicated for each MMCP. Functional categories include; 1. MT dynamics/stability, 2. Spindle checkpoints, 3. MT based motors, 4. Kinteochore-MT attachment, 5. Centrosome, 6. Protein destruction, 7. Uncharacterized, and 8. Not linked to spindle. MMCPs were analyzed for domain composition by querying Unison (http://unison-db.org). Proteins and domains were hierarchically clustered using the Pearson correlations of the numbers of each domain appearing in each protein. Results were visualized using Java TreeView (see Supplemental Experimental Procedures).

Table S2. Summary of MMCPs Domain Analysis, Related to Figure 1

Domain	# Proteins	Correlation Coefficient
Protein kinase	24	.48
Kinesin	21	.27
RRM 1	17	.44
Zinc finger, C2H2	15	.7
Ankyrin repeat	12	.48
Zinc finger, C3HC4	9	.4
Tubulin	7	.95

Notable clusters of proteins include those containing protein kinase, kinesin, RNA-binding, C2H2- and C3HC4-type zinc finger, ankyrin, and tubulin domains. The number of proteins in each cluster and the correlation coefficient of each cluster are indicated (for details see Supplemental Experimental Procedures).

Table S3. Screen Data and Statistical Analysis, Related to Figure 2

(for details see Supplemental Experimental Procedures).

Table S4. Summary of STARD9 siRNA Oligonucleotides, Related to Figure 5

Oligo	Target Sequence	% mRNA Depletion
STARD9-Pool		90
STARD9-1	GAGTTGCCAAAGGCTATAA	94
STARD9-2	TGCCAAAGGCTATAACATA	43
STARD9-3	CAACATGTAGTTACCAATT	38
STARD9-4	TCAACAGCTCAGTCAGCA	91

Indicated ON-TARGET*plus* siRNA (Dharmacon) oligonucleotides targeting STARD9 were used to transfect HeLa cells for 48 hours prior to cell harvesting and mRNA preparation. The percent of STARD9 mRNA depletion was determined by qRT-PCR, using TaqMan gene expression assay number Hs01397087 (Applied Biosystems).

Table S5. MMCP Gene Expression in Cancer, Related to Figure 5
MMCPs differential gene expression levels across 27 cancer tissues versus normal samples from the same tissue are indicated as log (base 2) expression ratios (for details see Supplemental Experimental Procedures).

Movie S1. siControl Cell Undergoing Mitosis, Related to Figure 7
Live time-lapse microscopy of control siRNA-treated cells. HeLa-GFP-H2B cells were treated with control siRNA for 24 hours, arrested with Thymidine for 18 hours, washed, and released into fresh media for 5 hours and filmed for 12 hours. Images were captured with a Zeiss Axio Imager.Z1 spinning disk confocal microscope and processed using SlideBook 4.2 (Intelligent Imaging) and converted to an Apple QuickTime movie. Each frame represents a five-minute interval.

Movie S2. siSTARD9 Cell Undergoing Mitosis, Related to Figure 7
Live time-lapse microscopy of STARD9-depeleted cells. Experiment was performed as described in Movie S1.

SUPPLEMENTAL EXPERIMENTAL PROCEDURES

Cell Culture and Synchronization

For all assays adherent HeLa cells were grown in F12:DMEM 50:50 medium (GIBCO) with 10% FBS, 2 mM L-glutamine and antibiotics, in 5% CO_2 at 37^o C. To obtain synchronized HeLa cells in mitosis, cells were treated with 300 nM nocodazole (Sigma-Aldrich) for 18 hours. To synchronize HeLa cells in G1/S, cells were treated with 2 mM Thymidine (Sigma-Aldrich) for 18 hours. For siRNA screens, cells were trypsinized and resuspended in F12:DMEM 50:50 medium (GIBCO) with 10% FBS, 2 mM L-glutamine and no antibiotics. For *in vivo* small molecule inhibition, cells were incubated with 100 μM Monastrol (Sigma-Aldrich) (Kinesin-5 inhibition), 200 nM compound 1 (GlaxoSmithKline) (Plk1 inhibition), 10 μM R0-3306 (EMD Chemicals), 5 μM taxol (microtubule stabilizer), or 300 nM Nocodazole (microtubule depolymerizer) six hours post thymidine release and fixed and stained four hours post small molecule addition. For gene knockdowns, cells were transfected with Dharmacon ON-TARGET*plus* siRNA (Non-Targeting Cat#D-001810-10, STARD9 Cat#L-008927-00, for custom STARD9 oligo sequences see Table S4), at 50 nM using Lipofectamine RNAiMAX (Invitrogen) for 48 hours prior to harvesting or fixation.

Mitotic Aster Microtubule Co-pelleting Assay

Mitotic aster microtubule co-pelleting assays were performed essentially as described in Mack and Compton, 2001. Four 15cm plates of nocodazole (300 nM for 18 hours) arrested mitotic HeLa cells were harvested by mitotic shake-off, washed in PBS plus 20 μg/ml cytochalasin B (Sigma-Aldrich) twice, washed with KHMD (78 mM KCL, 50 mM Hepes pH 7.0, 4 mM $MgCl_2$, 2 mM EGTA, 1 mM DTT, 20 μg/ml cytochalasin B) once

and resuspended in KHMDL (KHMD plus protease inhibitors leupeptin/pepstatin/chymostatin 1 μg/ml). Cells were dounce homogenized and extracts were cleared by ultracentrifugation at 38,000 RPM for 15 minutes. All steps were carried out at 4° C unless otherwise noted. Cleared lysates were supplemented with 5 μg/ml latrunculin B (Sigma-Aldrich) and 2.5mM ATP/AMP-PNP. Microtubule polymerization reactions were carried out in the presence of control vehicle DMSO or 10 μM taxol (Sigma-Aldrich) at 33° C for 30 minutes. Polymerization reactions were layered onto a 50% W/V sucrose/KHM cushion supplemented with 10 μM taxol for reactions with taxol-stabilized microtubules. Layered reactions were centrifuged for 2 hours at 39,000 RPM in a TLS-55 (Beckman) swinging bucket ultracentrifuge rotor. Samples from the supernatant were placed in an equal volume of 2X protein sample buffer. The microtubule co-pelleting fractions were washed three times with KHM buffer and resuspended in 1X protein sample buffer. Supernatant (S) and pellet (P) samples were boiled for 5 minutes at 90° C, run on an 8% Tris-Glycine gel, transferred onto Immobulon-P membrane (Millipore) and probed with indicated antibodies. For large-scale aster microtubule preps, sixteen 15 cm plates of confluent mitotic HeLa cells were used to prepare extracts and aster microtubule pellets were processed as described below.

Preparation of Aster Microtubule Pellets and Peptide Identification by LC-MS/MS

Aster microtubule pellets were solubilized by addition of 30 μl Solution A (8 M urea, 20 mM methylamine, 1 M LiCl, 2 mM EDTA in 100 mM pH 8.5 Tris-HCl). Solubilized pellets were heated at 95° C in a sealed Eppendorf tube for 15 minutes followed by addition of: 1 μl of 0.5 M dithiothreitol (DTT) and incubation for 2 hours at room

temperature, 3 μl of 0.5 M iodoacetamide and incubation for 2 hours in the dark at room temperature, 1 μl of 0.5 M DTT and incubation for 1 hour in the dark at room temperature, and 25 μl distilled water to dilute the 8 M urea to 4 M. Solubilized samples were treated with 60 μl of 10 mM $CaCl_2$ (pH 8.5) to stabilize trypsin, followed by the addition of 20 μl of 0.5 μg/μl trypsin (1:10 enzyme/total protein) and incubation at 37^{o} C for at least 12 hrs. Addition of trypsin was repeated and 1μl of acetic acid was added to stop the digest. Samples were stored at -80^{o} C. Digested sample solutions were diluted with water-0.1% trifluoroacetic acid (TFA) and loaded onto a microbore C18 guard column on an hplc. The urea and salt were rinsed off the column with water-0.1% TFA. The peptides were eluted with a step elution of 80% acetonitrile-0.1% TFA, collected manually in an Eppendorf tube and stored until examination by mass spectrometry. Mass Spectrometry and peptide identification was performed as described in (Vanderwerf et al., 2009) and proteins identified in the control sample, no taxol addition, were subtracted from those identified in the experimental sample, plus taxol.

Protein Domain Analysis

MMCPs were analyzed for domain composition by querying the Unison (http://unison-db.org) (Hart and Mukhyala, 2009) database, which calculates the presence of domains from the Pfam (Finn et al., 2008) and Prosite (Hulo et al., 2006) databases, as well as from signal sequence and transmembrane prediction algorithms. Proteins and domains were hierarchically clustered (Eisen et al., 1998) using the Pearson correlations of the numbers of each domain appearing in each protein. Results were visualized using Java TreeView (Saldanha, 2004).

Gene Expression in Cancer

Differential gene expression levels of genes in the MMCP were analyzed across 27 cancer tissues versus normal samples from the same tissue. Each tissue type was represented by 20 to >100 cancer and 2 to 20 normal samples. Microarray data were collected using the HG-U133 human chip (Affymetrix, Santa Clara, CA) and intensity data was collected and normalized using the MAS5.0 algorithm (Hubbell et al., 2002). For each of the 1055 probes corresponding to a protein in the MMCP set, within each tissue a t-test resulted in a p-value for the hypothesis that mRNA expression for that probe was different between cancer and normal samples. Probes with p-values greater than 0.01 in a given tissue had their cancer:normal ratios set to unity for that tissue. Expression ratios were log (base 2) transformed and clustered hierarchically along both probe and tissue axes using uncentered Pearson correlations. The clustered data were visualized as a heat map; red representing over-expression, green under-expression, and black no significant change in expression, for cancer relative to normal samples.

Construction of siRNA Library Targeting MMCPs

Dharmacon ON-TARGET*plus* siRNA smart pools and individual oligos targeting the MMCP gene set were arrayed on 96 well plates. In total 592 genes were targeted with 592 OTP pooled oligos and 2,368 individual oligos. Columns 1 and 12 of each 96 well plate were reserved for control siRNAs.

Screen Conditions

For transfection, Oligofectamine (Invitrogen) in OPTI-MEM (Invitrogen) was added to each well of a 96 well plate (black with clear bottom, poly-D-Lysine coated, Beckton Dickinson Labware) containing the prespotted siRNA library. The mixture was incubated for 40 minutes and HeLa cells, 10,000 cells/well, were plated onto the siRNA mixture using a multidrop combi (Thermo Scientific) to ensure even distribution. Cells were incubated at 37^{o} C for indicated times. For + taxol screens, taxol (100 nM final concentration) was added to each well 24 hours post transfection using a RapidPlate liquid handler (Caliper Life Sciences) and cells were incubated for an additional 18 hours (42 hours total). Cells were fixed by paraformaldehyde (4% final concentration) perfusion for 15 minutes at room temperature. Following fixation, cells were permeabilized with .2% Triton X-100/PBS for 5 minutes at room temperature. Plates were washed with PBS one time and stained for phospho-histone H3 and DNA (1:50 Alexa 488 phospho-histone H3 (Ser10) (Cell Signaling) and 1 μg/ml Hoechst 33342 in 5% fish gelatin (Invitrogen) for 1 hour. After staining plates were washed two times with .1% Triton X-100/TBS and preserved in 50% glycerol at 4^{o} C until imaging. All washes were carried out with a BioTek microplate washer ELx405 (BioTek Instruments) equipped with a microplate stacker.

Image Based Data Capture and Processing

Screen plates were imaged on a Cellomics ArrayScanVTI HCS Reader (Cellomics) automated inverted fluorescence microscope equipped with a microplate stacker. The ArrayScan/vHCS:Scan software was used for image acquisition using the following parameters: objective: 10X .5 NA, bio application algorithm: Spot Detector, number of channels: two Hoechst and FITC, focus channel: Hoechst, scan limits: 1000 objects

(nuclei), with background correction and object segmentation on. Data was analyzed using ArrayScan/vHCS:View software and exported to Excel spreadsheets.

Statistical Analysis

For both percent mitotic index (MI) and apoptotic index (AI) data, test oligos were compared with either the distribution of the control oligos, or the distribution of all the oligos. The distributions are characterized by the mean values and standard deviation. For mitotic index data, the mean and standard deviation of the MI in log scales from control oligos are computed. Then the MI from the test oligos are compared with the mean ± one standard deviation way from the mean and mean ± 2 standard deviations away from the mean. For normalized mitotic indices and apoptotic indices scores, the mean and standard deviations of the values in log scales are computed, and then the values of the test oligos are again compared with the mean ± one standard deviation way from the mean and mean ± 2 standard deviations away from the mean. To correlate MI and AI screens, normalized MI and AI values were visualized for each individual oligo simultaneously. Scatter plots were generated with solid lines representing the mean, dashed lines representing mean ± one standard deviation, and dotted lines representing mean ± 2 standard deviations of all MI or AI values. Plots, mean values, and standard deviation calculations are in log scale. Codes are available upon request.

STARD9 Gene Expression

500 ng of mRNA was prepared from indicated tissues and the relative STARD9 mRNA levels compared to PPIB were quantified using the QuantiGene Reagent System as

described by the manufacturer (Panomics). qRT-PCR was carried out using the STARD9 (Hs01397088_m1) and GAPDH (402869) probes (Applied Biosystems).

STARD9 Motor Domain Assays

For STARD9 motor domain expression (modified from Moyer et al., 1996), microtubule-binding assays (as described in Goode and Feinstein, 1994), centrosome binding assays (as described in Mitchison and Kirschner, 1986), ATPase assays (as described in Funk et al., 2004), localization studies, and rescue experiments, the first 387 amino acids of STARD9 (wild type, T110N mutant, and R223A mutant) were fused to the C-terminus of either GST (pGEX-6P vector) or EGFP (pGLAP1 vector (Torres et al., 2009). For localization, overexpression, and rescue experiments, EGFP control, or EGFP-tagged STARD9-MD-WT, T110N, or R223A were transfected in to HeLa cells for the indicated times. Cells were fixed and stained for DNA, α-tubulin, EGFP, and pericentrin. For centrosome binding experiments, 100 μg of GST-STARD9-MD or GST-Skp1, were pre-bound to glutathione agarose beads, and incubated with 500 μg of mitotic centrosome preps, after 1 hour beads were pelleted and washed three times with 110mM NaCl, 5mM ATP, 80mM PIPES pH 6.9, 5mM MgCl2, 1mM EGTA, and samples from the first supernatant and the pellet fraction were resolved by SDS-PAGE and analyzed by immunoblot analysis with indicated antibodies.

TUNEL Fluorometric Assay

The DeadEnd fluorometric TUNEL system (Promega) was used to measure DNA fragmentation as described by manufacturer. Briefly, siControl and siSTARD9 cells were synchronized in G1/S with 2 mM Thymidine for 18 hours, washed, released, and

fixed with 4 % paraformaldehyde for 10 minutes at 37^{o} C six hours post mitotic entry. DNA breaks were labeled with a nucleotide mix containing fluorescein-12-dUTP and rTdT enzyme for one hour at 37^{o} C. The reaction was stopped by addition of 2x SCC and the DNA was visualized by staining with Hoechst for 10 minutes.

Live Time-lapse Microscopy

16 hours post RNAi treatment HeLa-GFP-H2B cells were arrested with 2 mM Thymidine for 18 hours, washed, and released into fresh media. Cells were imaged live at 63X magnification 5 hours post release for 12 hours. Images were captured with a Zeiss Axio Imager.Z1 microscope and processed using SlideBook 4.2 (Intelligent Imaging) and converted to an Apple QuickTime movie. Each frame represents a five-minute interval.

Panels of Cancer Cell Lines

The following cancer cell lines were used to analyze STARD9 expression levels and depletion phenotype. Panel of skin cancer cell lines in order of appearance in Figures 5F and 5G, M395, M275, M202 (L), M368, M257, M244 (K), M243 (H), T47D HE, EFM19 HE, 361 HE. Panel of lung cancer cell lines in order of appearance in Figures 5F and 5G, MCI H460, H520, H441, H1703, A549, H157-S, H292, RH2, H358, H596.

Antibodies

The following antibodies were used: α-tubulin (Serotec), γ-tubulin (Sigma), Kinesin-5 (Cytoskeleton Inc), STARD9 (Santa Cruz), Aurora B (BD Transduction), Plk1 (Zymed), NuMA and TPX2 were gifts from Duane Compton, centrin and pericentrin were gifts from Jeffrey Salisbury, BubR1 and Bub1 were gifts from Hongtao Yu, INCENP was a

gift from Wei Jiang, Crest was a gift from Bill Brinkley, and Centrobin was a gift from Qingshen Gao. FITC-, 488-, Cy3- and Cy5-conjugated secondary antibodies were from Jackson Immuno Research (Affinipure), and Molecular Probes.

SUPPLEMENTAL REFERENCES

Eisen, M.B., Spellman, P.T., Brown, P.O., and Botstein, D. (1998). Cluster analysis and display of genome-wide expression patterns. Proc Natl Acad Sci U S A *95*, 14863-14868.

Finn, R.D., Tate, J., Mistry, J., Coggill, P.C., Sammut, S.J., Hotz, H.R., Ceric, G., Forslund, K., Eddy, S.R., Sonnhammer, E.L., *et al.* (2008). The Pfam protein families database. Nucleic Acids Res *36*, D281-288.

Funk, C.J., Davis, A.S., Hopkins, J.A., and Middleton, K.M. (2004). Development of high-throughput screens for discovery of kinesin adenosine triphosphatase modulators. Anal Biochem *329*, 68-76.

Goode, B.L., and Feinstein, S.C. (1994). Identification of a novel microtubule binding and assembly domain in the developmentally regulated inter-repeat region of tau. J Cell Biol *124*, 769-782.

Hart, R.K., and Mukhyala, K. (2009). Unison: an integrated platform for computational biology discovery. Pac Symp Biocomput, 403-414.

Hubbell, E., Liu, W.M., and Mei, R. (2002). Robust estimators for expression analysis. Bioinformatics *18*, 1585-1592.

Hulo, N., Bairoch, A., Bulliard, V., Cerutti, L., De Castro, E., Langendijk-Genevaux, P.S., Pagni, M., and Sigrist, C.J. (2006). The PROSITE database. Nucleic Acids Res *34*, D227-230.

Mack, G.J., and Compton, D.A. (2001). Analysis of mitotic microtubule-associated proteins using mass spectrometry identifies astrin, a spindle-associated protein. Proc Natl Acad Sci U S A *98*, 14434-14439.

Mitchison, T.J., and Kirschner, M.W. (1986). Isolation of mammalian centrosomes. Methods Enzymol *134*, 261-268.

Moyer, M.L., Gilbert, S.P., and Johnson, K.A. (1996). Purification and characterization of two monomeric kinesin constructs. Biochemistry *35*, 6321-6329.

Saldanha, A.J. (2004). Java Treeview--extensible visualization of microarray data. Bioinformatics *20*, 3246-3248.

Torres, J.Z., Miller, J.J., and Jackson, P.K. (2009). High-throughput generation of tagged stable cell lines for proteomic analysis. Proteomics *9*, 2888-2891.

Vanderwerf, S.M., Svahn, J., Olson, S., Rathbun, R.K., Harrington, C., Yates, J., Keeble, W., Anderson, D.C., Anur, P., Pereira, N.F., *et al.* (2009). TLR8-dependent TNF-(alpha) overexpression in Fanconi anemia group C cells. Blood *114*, 5290-5298.

Vilella, A.J., Severin, J., Ureta-Vidal, A., Heng, L., Durbin, R., and Birney, E. (2009). EnsemblCompara GeneTrees: Complete, duplication-aware phylogenetic trees in vertebrates. Genome Res *19*, 327-335.